# Hazard and vulnerability in urban inundated underground space: Hydrodynamic analysis and risk assessment of evacuation staircase

Qijie Li[a], Junqiang Xia[a,*], Zhihua Xie[b], Meirong Zhou[a], Shanshan Deng[a]

[a]*State Key Laboratory of Water Resources and Hydropower Engineering, Wuhan University, Wuhan, 430072, China*
[b]*School of Engineering, Cardiff University, Cardiff, CF24 3AA, United Kingdom*

**Abstract**

Underground flooding events are being exacerbated due to the rapid expanding of underground space in urban and the extreme precipitation events by climate change. It is increasingly necessary to have a more accurate understanding of hydrodynamics and instability of human on the staircase in flood-prone area for metro system design and risk identification. However, the turbulent complexity and complicated fluid dynamics challenge the study of flow structure and the calibration of human instability model. The focus of this work is to study fluid dynamics and to analyze human instability on the staircase in flood area based on the volume of fluid method incorporated with the mechanics-based method. Flow characteristics and representative human positions on the staircase are considered. Firstly, comparisons between numerical and experimental results are used to verify the capacity of the numerical simulation in capturing velocity, pressure field and flow structure. Secondly, numerical results of flow over the staircase with three representative human locations are carried out and a critical hydraulic jump region of human instability is demonstrated. When human located in the hydraulic jump region or on the rest platform, vortical flow structures in the vicinity of human body were obviously enhanced by the intensified turbulence. While the influence of flow characteristic is reduced when human on the upper bench of the staircase. In addition, the instability difference in hydraulic jump region between an adult and a child is discussed. It is noted that the presented study can providing a way to study fluid mechanics and analyze the loss of human stability on the staircase in underground space. Overall, the work demonstrates the potential for further use to support flood risk management in metro system.

*Keywords:* Urban flooding, Human instability, Hydrodynamics, Risk assessment, Underground space

## 1. Introduction

Metro systems perform a significant function of urban transportation worldwide due to the rapid globalization and urbanizing process in the last decades. Urban passengers rely on a secure, reliable, and accessible underground service for their regular conveyance (Forero-Ortiz and Martnez-Gomariz 2020). However, many cities were inundated by urban floods, and some flooded water intruded into underground spaces (Zhou et al. 2017, Sun et al. 2021). Flood hazards can restrict normal metro service and lead sever threaten of people's safety and economic damage (Ishigaki et al. 2009, Jiang et al. 2014, Lyu et al. 2018, Lyu et al. 2019, Valdenebro and F.N. Gimena 2019). Due to

*Corresponding author
*Email address:* xiajq@whu.edu.cn (Junqiang Xia)

the increase of urban waterlogging, a series of urban design strategies and management polices were created for urban drainage system to optimize the Sustainable Flood Retention Basin (SFRB) assessment in practice (Deng et al. 2013; Emanuelsson et al. 2014; Mugume et al. 2015; Campisano et al. 2017; Shao et al. 2017; Xu et al. 2018; Motta et al. 2021; Zinda et al. 2021; Singh et al. 2018; Kramer et al. 2016).

Although a great number of efforts have been made by researchers and governments, destructive flooding events in mega-cities still challenge us(Choi et al. 2021; Eini et al. 2020; Tanir et al. 2021; Park and hun Won, 2019; Li et al. 2019). The inundation in underground space is one of the urgent need to reduce the damage from severe inundation of underground facilities (Lyu et al. 2018; Wu et al. 2018; Lyu et al. 2019). A large number of urban underground facilities including metro-systems and shopping malls have been constructed to accelerate economic development and human transportation (Tan et al. 2017; Shen et al. 2017; Kim et al. 2017; Tan and Lu, 2018). However, extreme flood events have caused catastrophic damage and contamination to those underground infrastructures, which threatens life security and degrades economic activities (Zhao et al. 2016; Qiao et al. 2017; Peng et al. 2018; Liu et al. 2021). Fig. 1 shows the flooded metro stations in Guangzhou and Wuhan, respectively.

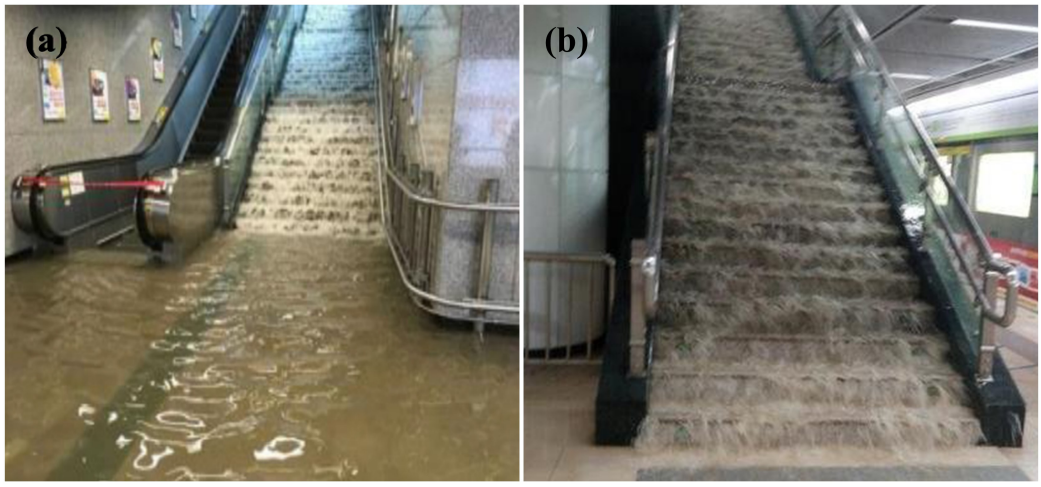


Figure 1: Metro station inundated during urban flooding. (a) Changpan station flooded on 10th May, 2016 in Guangzhou (Lyu et al. 2016); (b) Zhongnan station flooded on 6th July, 2016 in Wuhan.

To achieve cities sustainability, more attentions have been attracted to the flood-prone underground spaces, where water intrusion can cause severe damages on human beings, infrastructures, and urban functions (Kallianiotis et al. 2018). When urban flooding occurs, staircases are critical route for passenger evacuation. Flow over staircase is accelerating on a steep slope, which is characterized by a turbulent flow with fragmentation, splash, and hydraulic jump. The turbulent complexity and complicated fluid-mechanics make the physics complicated. Currently, a few studies have been done in literature and there is still a gap between the demands in practice and the effective methods for understanding and assessing the potential risk in a flood-prone metro-staircase region.

In general, either experimental or numerical approaches can be used to study flow over underground staircase and analyze human stability. Several experiments have been conducted to study the evacuation safety of people walk-

ing through a inundated staircase without rest platform (Ishigaki et al. 2006 Ishigaki et al. 2009). Although experimental tests are able to identify specific conditions of human evacuation performance on flooding staircase (Ishigaki et al. 2006 Ishigaki et al. 2009 Shao et al. 2015), fluid-mechanics and human instability details need to be studied further. Computational fluid dynamics (CFD) has been developing rapidly with the advancement of computer technology and numerical methods over the past decades. Nowadays, CFD is widely used in the study of compressible and incompressible flows and has become an indispensable tool in engineering applications. This framework provides an alternative way to study the flow over staircase and to evaluate the risk of human instability(Shao et al. 2015 Arrighi et al. 2017 Jiang et al. 2014). The numerical simulation of incompressible two-phase flows requires a technique to identify the boundary between the two fluids, as this boundary is not known beforehand (Jafari and Ashgriz 2013). Among the phenomena that need to be handled are topological changes of the interface, discontinuities, coalescence, and breakup. Several interface modelling techniques have been developed to tackle complex fluid flows. The Volume-of-Fluid method (Hirt and Nichols 1981) uses a volume fraction function to indicate the quantity of each fluid in each cell and is very popular among researchers (Scardovelli and Zaleski 1999). VOF methods have benefited from continuous improvement over decades due to its popularity among researchers in the field of interface capturing. Firstly, the mass in VOF is conserved naturally due to the development of an advection algorithm based on a discrete representation of the conservation law. Secondly, the extension of VOF from 2D to 3D is relatively straightforward. Moreover, the domain decomposition of VOF for parallel implementation is relatively simple.

When flow over the staircase, a sharp interface exists due to the large density ratio difference between water and air. The stability and accuracy of the method to define the sharp interface for the incompressible two-phase flow problem proved to exert an essential effect on the numerical simulation of flow structures. Based on the VOF method, (Yoneyama et al. 2009) simulated the flow over a staircase with coarse mesh, which results in a less velocity value compared to the experimental results. Typically, a staircase in metro system is divided into several segments by rest platforms. The existence of a rest platform significantly influents the flow characteristics and cause a hydraulic jump downstream the platform, which affect the human stability on the staircase in flood-prone area (Shao et al. 2015). It is also found that the existence of a rest platform in a straight-run type staircase can dramatically influence the hydrodynamic force (Jiang et al. 2014). Therefore, it is essential to identify hydrodynamics and understand human instability mechanisms for management strategies and emergency planning.

Generally, the instability mechanisms can be classified into sliding (friction instability) and toppling (moment instability). Sliding instability occurs when the flow induced drag force is larger than the frictional force between human feet and the substrate surface (Keller and Mitsch 1993). Sliding instability prevailed in high-flow velocities and low water depths. Toppling happens when the flow induced moment exceeds the resisting moment of the effective weight of the body (Abt et al. 1989, Jonkman and Penning-Rowsell 2008). Toppling instability is crucial for high water depths (Abt et al. 1989). Research methods of these instability mechanisms can be divided into two categories. One approach is to obtain regressed relations based on laboratory experiments. In this approach, there exist a wide range of criteria for human instability in floodwaters due to effect of non-hydraulic parameters, including physical characteristics and psychological factors. Another approach comprises experimental or theoretical formulae derived from a mechanics-based

analysis (Cox et al. 2010). This type of criterion only considering the hydrodynamic conditions, which is independent of people's physical and psychological attributes. (Xia et al. 2014a, 2014b, Falconer et al. 2015) derived two formulae in calculation of the critical incipient velocity for both sliding and toppling instability, which can account for the effect of body buoyancy and the influence of a non-uniform upstream velocity profile on the stability of the human body. However, these formulae cannot be used directly for the stability analysis on the staircase due to the difference of physical model (e. g. slope, steps, and rest platform) and complicated hydrodynamics (e. g. hydraulic jump). Thus, it is necessary to further study human stability on the staircase with flood waters based on the theoretical, experimental, and numerical studies.

The aim of this work is to study hydrodynamics and human stability of a flow over the staircase with different representative human locations and body shapes. A 3D numerical model is proposed based on the VOF method and a synthetic identification of the high danger zone is made based on a mechanics-based analysis and the safety index map on the staircase. This paper is organized as follows: In section 2, a brief introduction of the flow governing equations and an explanation of the numerical method are given. Two validation benchmark tests are conducted to verify the capability of the numerical simulation. Subsequently, the mechanics-based analysis of human instability in the region of flow over the staircase is presented in section 3. In section 4, numerical simulation of flow over the staircase with three representative human locations are carried out. Human instability analysis on the staircase especially in hydraulic jump region are demonstrated based on the results of flow characteristic distribution and the critical instability conditions. Finally, we summarize the paper with conclusions in Section 5.

## 2. Model description and validation

### *2.1. Governing equations*

The fluid motion of an incompressible, immiscible, isothermal flow can be mathematically described by the continuity and momentum differential equations as:

$$\nabla \cdot \mathbf{u} = 0, \tag{1}$$

$$\rho \left( \frac{\partial \mathbf{u}}{\partial t} + \mathbf{u} \cdot \nabla \mathbf{u} \right) = -\nabla P + \nabla \cdot \tau_s + \rho \mathbf{g} + F_\sigma, \tag{2}$$

where $\rho$ is density, $\mathbf{u} = (u, v, w)$ is velocity, $P$ is the pressure, $F_\sigma$ is the surface tension force, $\mathbf{g}$ is the gravitational acceleration, and $\tau_s$ is the viscous stress tensor.

### *2.2. Volume of Fluid Method (VOF)*

The VOF method was first introduced by Noh and Woodward in 1976 (Noh and Woodward 1976), and developed by Hirt and Nichols [13]. The VOF function $\alpha$ is defined such that it is unity at any point occupied by fluid, and zero otherwise. The average value of $\alpha$ in a cell would then represent the fractional volume of that cell occupied by fluid, as demonstrated in Fig. 2. Cells with $\alpha$ values between 0 and 1 must therefore contain an interface. In VOF method, a

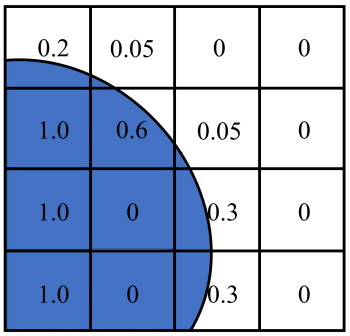


Figure 2: Schematic of a fluid distribution in a 2-D Cartesian grid with its accompanying indicator $\alpha$ values

transport equation is solved to determine the value of the fluid fraction throughout the computational domain (Hirt and Nichols, 1981) as follows:

$$\alpha_t + \nabla \cdot (\mathbf{u}\alpha) = 0, \tag{3}$$

and the physical properties of the immiscible fluids are calculated as such;

$$\rho = \rho_L \alpha + \rho_G (1 - \alpha), \tag{4}$$

$$\mu = \mu_L \alpha + \mu_G (1 - \alpha). \tag{5}$$

It is important to remark that VOF method considers both fluids, the transport of other properties is treated by means of weighted averages, according to the fluid fraction in each mesh element. VOF method has been successfully applied to various problems and high order differencing schemes are designed to overcome interface deformation deficit false. In this work, the VOF method coupled with large eddy simulation model is applied in Flow-3D to simulate flow over the staircase with a rest platform when human located on different parts of the staircase. The coupling of velocity and pressure was achieved by the implicit Successive Over Relaxation (SOR) method. Concerning time discretization, the time step length is automatically adjusted in order to ensure that Courant numbers remain below a threshold of $C_r < 0.75$. A mesh sensitivity analysis has been made for the numerical simulation of flow over the staircase with human on it. Four different mesh sizes (0.005 m, 0.0075 m, 0.001 m, 0.0015 m) in the vicinity of human have been tested to assess the grid sensitivity on the accuracy of the numerical model. The difference of mesh size 0.005 m an 0.01 m in the estimated average coefficients of drag and lift was within a small margin of error. Accordingly, the 0.01 m was used in this study for computational efficiency. The total number of cells is about $1.8 \times 10^6$ and the maximum size in the whole mesh domain is 0.025 m.

### *2.3. Validation of the numerical model*

In this section, two test cases are conducted to verify the numerical model including flow over straight-type staircase with and without the rest platform. Numerical simulation results are compared to the experimental data from Tokyo University(Ishigaki et al. 2006) and Zhejiang University(Shao et al. 2015).

### 2.3.1. *Straight-type staircase test*

In Fig. 3, flow over a straight-type staircase experiment was conducted in Tokyo university (Ishigaki et al. 2006) using a water tank, a pump, a channel, and a physical staircase model. The configurations of this experiment are illustrated in Fig. 3. The height and the length of the staircase model are 3m and 6m, respectively. The corresponding slope is 1:2 with an angle of $26.6^o$. The width of the staircase is 1.0m. The staircase consists of 20 steps and each step has a 0.15m height and 0.3m length.

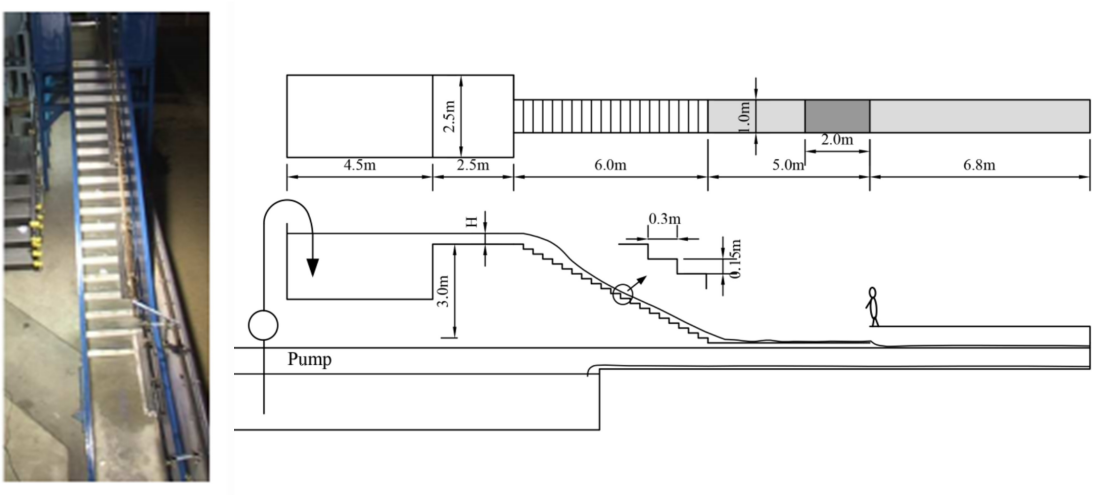


Figure 3: Experiment configurations of straight-type staircase test (Ishigaki et al. 2006).

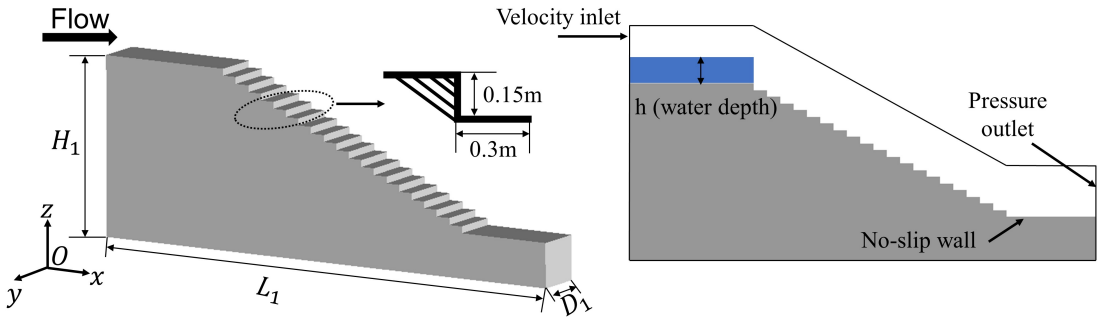


Figure 4: Numerical simulation configurations and boundary conditions of straight-type staircase test.

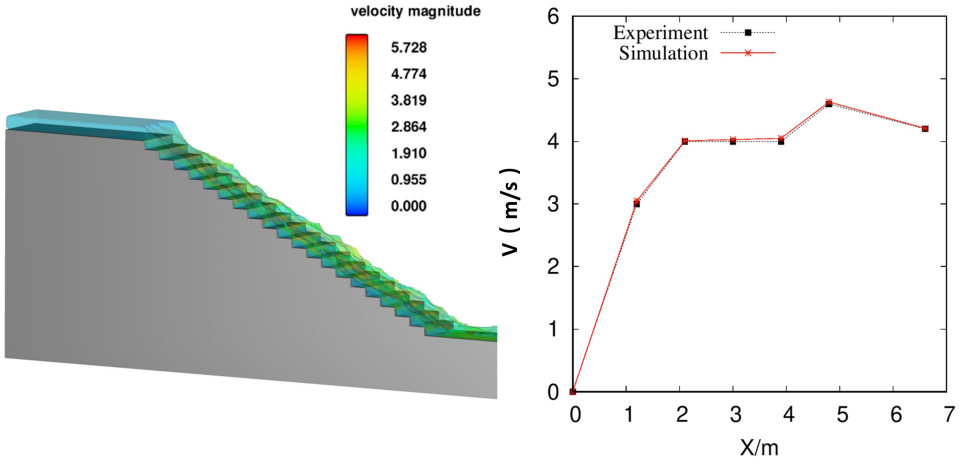


Figure 5: Flow velocity distribution on the staircase. A comparison between numerical simulation and experiment.

Fig. 4 demonstrates the numerical simulation configurations and boundary conditions. $L_1 = 7.0$ m, $H_1 = 3.0$ m, and $D_1 = 1.0$ m. Fig. 5 shows the results of flow velocity distribution with initial water depth 0.3m. Comparing the simulations with experimental data, the velocity distribution agrees well with test value.

### 2.3.2. *Straight-type staircase with rest platform test*

In this subsection, flow over a straight-type staircase with a rest platform experiment was conducted in Zhejiang university (Shao et al. 2015) as shown in Fig. 6 . This experiment was conducted based on a 1:2 scaled physical model, which consists of 26 identical steps (with the height $h = 0.08$ m and the length $l = 0.14$ m). The pseudo-bottom inclination angle of the staircase is $29.7^o$, corresponding to a slope of 1:1.75. The width of the staircase is 0.8 m. The rest platform is located in the middle of the staircase and divide the staircase into upper and lower segments.

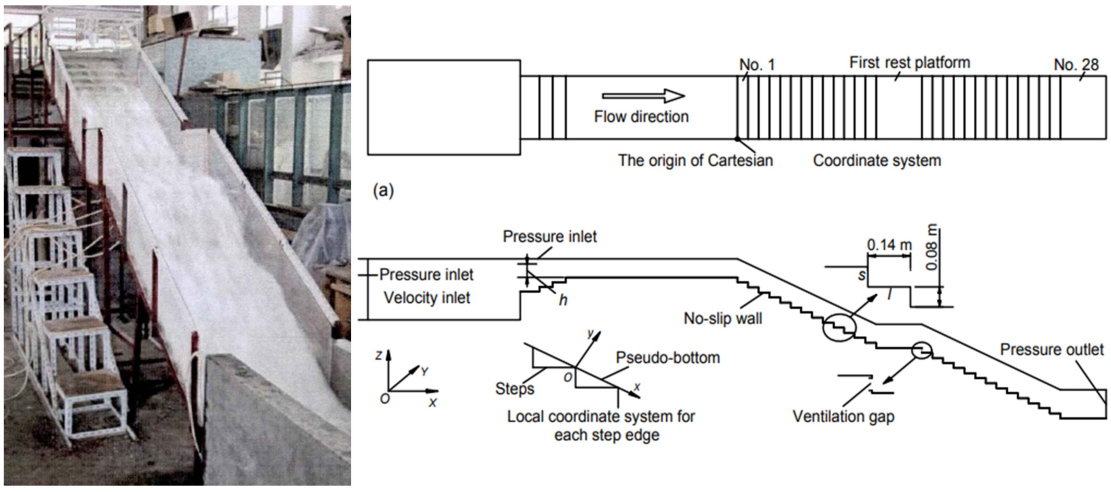


Figure 6: Experiment configurations of straight-type staircase with a rest platform test (Shao et al. 2015).

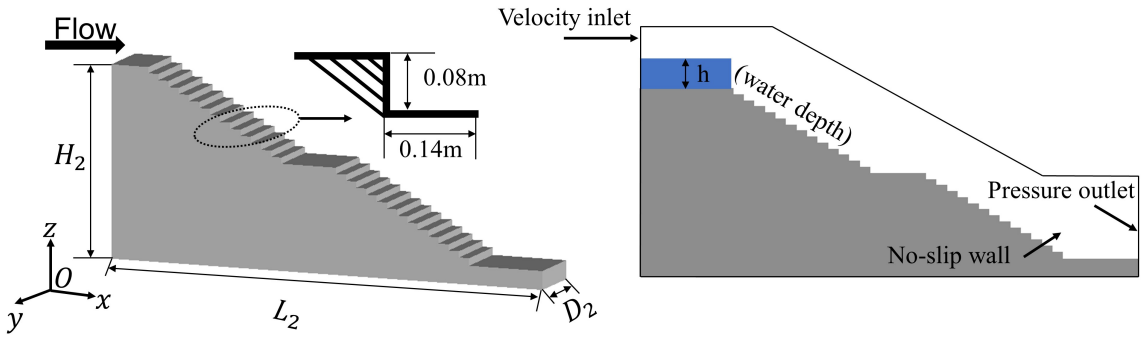


Figure 7: Numerical simulation configurations and boundary conditions of straight-type staircase with a rest platform.

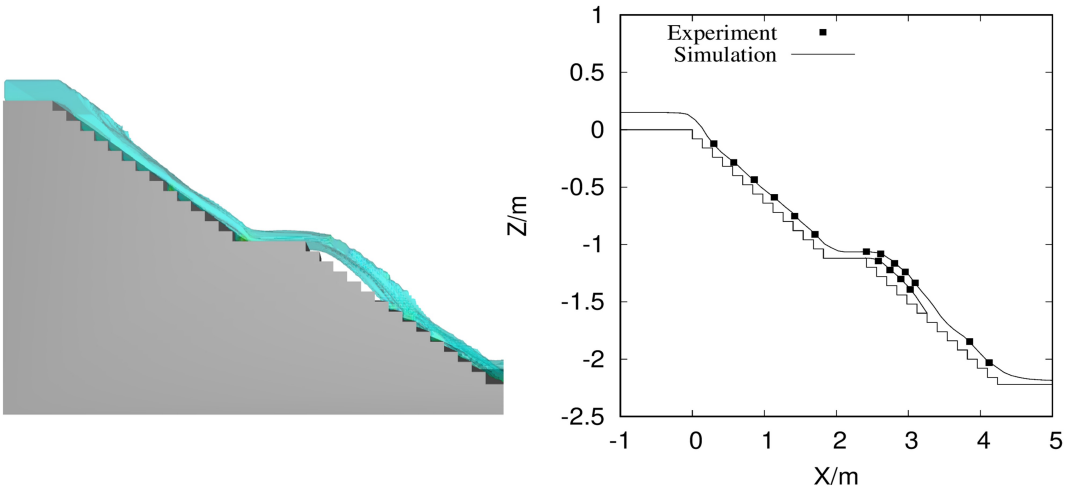


Figure 8: Air-water interface on the staircase obtained by simulation and experiment.

Numerical simulation configurations and boundary conditions are illustrated in Fig. 7. $L_2 = 6.0$ m, $H_2 = 2.5$ m, and $D_2 = 0.8$ m. Fig. 8 shows the results of flow surface elevation in the simulated region. Results reveal that the numerical simulation captures flow surface elevation accurately compared to the experimentally measured data. It provides the detailed verification of the ability of the proposed numerical framework to describe both velocity fields and flow structure.

## 3. Methodology of mechanics-based analysis of human instability

In this section, a mechanics-based method is used for human stability hydrodynamic analysis. Generally, there are two potential instability mechanisms including sliding (friction) and toppling (moment) instability as show in Fig. 9, when considering the stability of a human body in flood waters (Xia et al. 2014b). To analysis the instability conditions of a human body on stairs in flood-prone underground area, a geometric description of the human body and a sketch of all the forces acting on a flooded human body is given as follows.

### 3.1. Geometric representation of the human body and acting forces

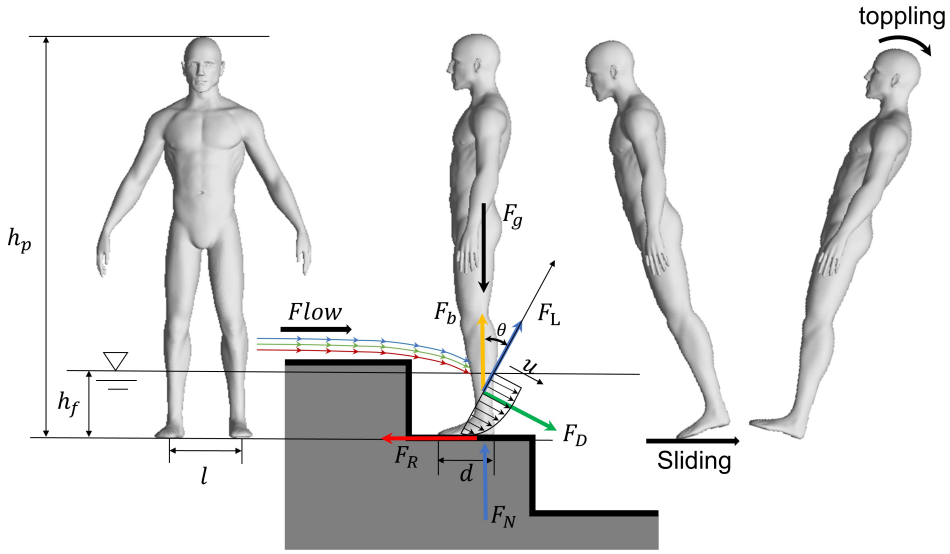


Figure 9: Geometric structure of human body and acting forces.

Fig. 9 shows the sketch of all the forces acting on a flooded human body for friction and moment instability on steps, respectively. $F_D$ is the drag force of the flow and $F_R$ is the frictional force between human feet and the step surface. $F_g$ is the human gravitational force, $F_b$ is human buoyancy force, $F_L$ is human lift force, and $F_N$ is the normal reaction force from ground. $h_p$ is human height and $h_f$ is flowing water depth over feet on the step. $\theta$ is the angle of force $F_L$ in vertical direction. To simplify the geometric parameters, the shape of the human body is mechanically schematized in Fig. 9, with reference to an approximate prism of height $h_p$, width $l$ and length $d$ (Lind et al. 2004). Thus the acting forces on human body can be expressed as follows:

$$F_g = \rho_p \cdot g(h_p \cdot d \cdot l), \tag{6}$$

$$F_b = \rho \cdot g(h_f \cdot d \cdot l), \tag{7}$$

$$F_D = \frac{1}{2}\rho_p U^2 C_D(h_p \cdot l), \tag{8}$$

$$F_L = \frac{1}{2}\rho_p U^2 C_L(h_p \cdot l), \tag{9}$$

$$F_R = \mu F_N = \mu(F_g - F_b + F_D \cdot sin\theta - F_L \cdot cos\theta). \tag{10}$$

### 3.2. Instability conditions of a human body on staircase in flood flows

The critical conditions of instability formula for human instabilities on the staircase are described as follows:

(1) Critical condition for sliding instability

$$F_R = F_D \cdot cos\theta + F_L \cdot sin\theta. \tag{11}$$

Substituting Eq. (8)and Eq. (10) into Eq. (11), the critical condition for human sliding instability can be obtained as follows:

$$2\mu d\left(\frac{\rho_p}{\rho} - \frac{h_f}{h_p}\right) = \frac{U^2}{g}\left\{cos\theta \cdot (C_D + C_L) - sin\theta \cdot (C_D - C_L)\right\}. \tag{12}$$

(2) Critical condition for toppling instability

$$(F_g - F_b + F_D \cdot sin\theta - F_L \cdot cos\theta) \cdot d = (F_D \cdot cos\theta + F_L \cdot sin\theta) \cdot \frac{1}{2} h_f. \tag{13}$$

Analogously, substituting Eq. (6), Eq. (7), Eq. (8) and Eq. (9) into Eq. (11), the critical condition for human toppling instability can be obtained as follows:

$$2d^2\left(\frac{\rho_p}{\rho} - \frac{h_f}{h_p}\right) = \frac{U^2}{g}\left\{cos\theta \cdot (\frac{1}{2}C_D \cdot h_f + C_L \cdot d) - sin\theta \cdot (C_D \cdot d - \frac{1}{2}C_L \cdot h_f)\right\}. \tag{14}$$

## 4. Results and discussion

In this section, numerical simulations of flow over the staircase with three representative human locations are carried out. Numerical results are analyzed in terms of hydrodynamics and flow characteristics. A mechanics-based analysis for human instability in hydraulic jump region is given based on the critical instability conditions. Identification of hazard zones on the inundated staircase is made using a risk assessment index $f(U^2 \cdot h_f)$ (Ishigaki et al. 2006).

### 4.1. Hydrodynamics of flow over staircase with different human locations

Numerical simulations of free surface flows on steps are conducted based on a scaled (1:2) physical model of a straight-type staircase. The pseudo-bottom inclination angle is $26.6^o$, corresponding to a slope of 1:1.75. A rest platform is located in the middle of the staircase, and the staircase is divided into upper and lower segments. Each part composes 13 identical steps numbered sequentially from No.1 to No.13 from the top to the bottom of the staircase. The height $h$ of each step is 0.08m and the length $l$ is 0.14m.

#### 4.1.1. Case 1: Human on the rest platform of the underground staircase

Fig. 10 shows the configurations of human location on the rest platform of the staircase. $L_3 = 6.0$ m, $H_3 = 2.5$ m, and $D_3 = 1.2$ m. In this case, the flow velocity on the upstream staircase increased gradually from the ground entrance to the rest platform. When water flows through the intermediate rest platform, due to the sudden increase in the horizontal length, the relatively stable flow pattern of falling water, transitional water and sliding water upstream of the platform is destroyed.

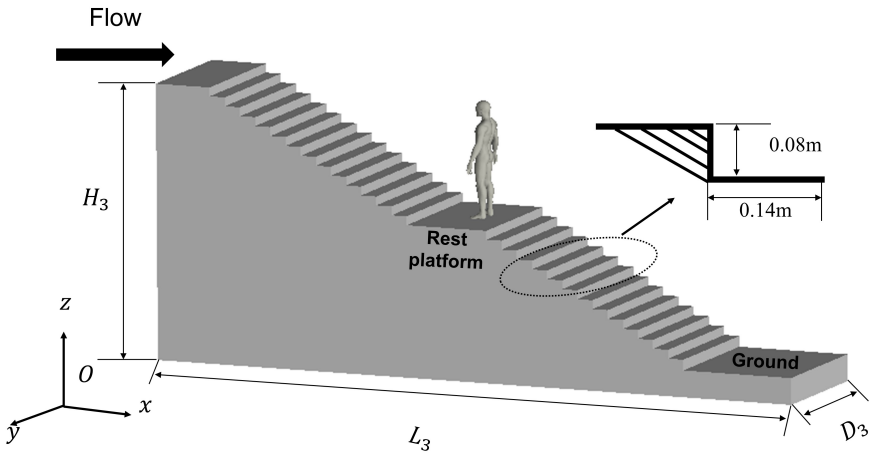


Figure 10: Configurations of human on the rest platform of the staircase.

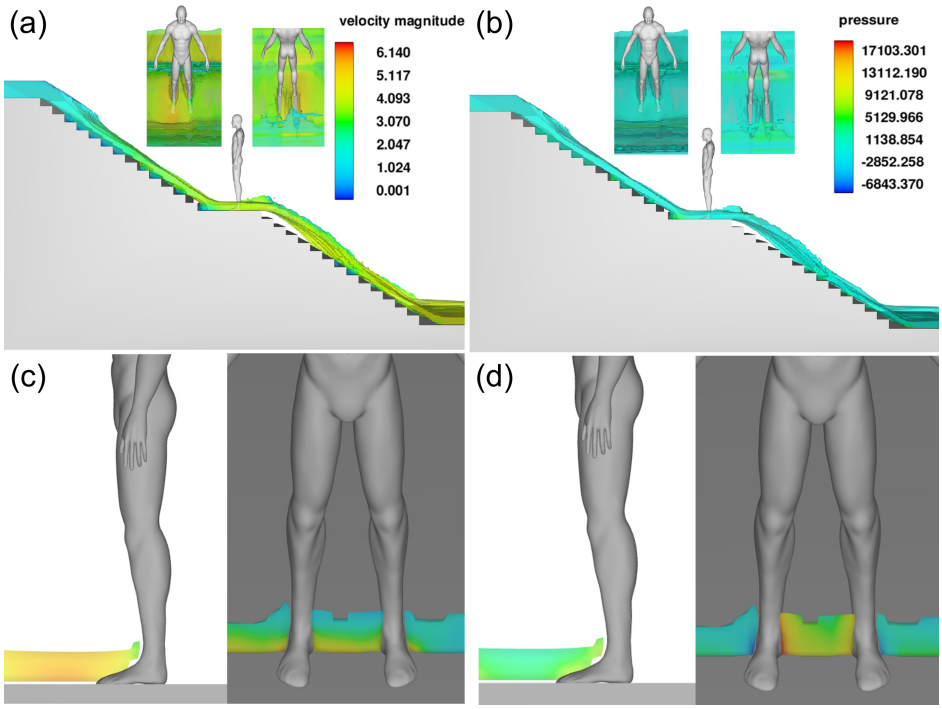


Figure 11: Flow structure including velocity and pressure of human on the rest platform of underground staircase. (a) distribution of velocity, (b) distribution of pressure, (c) amplified view of velocity in the vicinity of human body, (d) amplified view of pressure in the vicinity of human body.

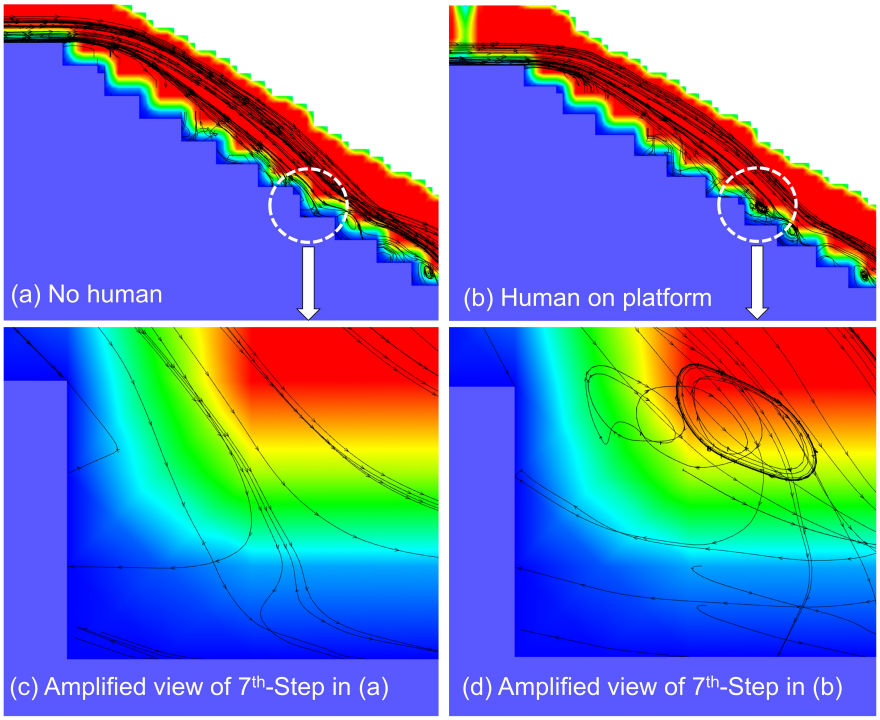


Figure 12: Flow streamline distribution in the lower bench of the staircase. (a) No human on the staircase, (b) Human on the platform, (c) Amplified view of flow streamline distribution near the 7-th step downstream of the platform in (a), (d) Amplified view of flow streamline distribution near the 7-th step downstream of the platform in (b).

Fig. 11 depicts the simulated flow with velocity magnitude and pressure distribution on the staircase and the amplified view of related results around the human body on the rest platform. It is observed that the free surface elevation decreases downstream after passing the ankles where the flow accelerates. A significant hydraulic jump occurred after the rest platform. This is because when water flows through the intermediate rest platform, due to the sudden increase in the horizontal length of the intermediate rest platform steps, the relatively stable flow pattern of falling water, transitional water and sliding water upstream of the platform is destroyed, and the downstream of the platform will produce a jet stream, and the water tongue will break away. The step surface is exposed to the air, creating a jet flow cavity in the lower part of the hydraulic jump.

When the flow reaches to human on the platform, the upstream flow is slightly decelerated due to the obstruction of the human body and the downstream velocity increased vice-versa. The pressure increased on the inner side of the feet and above the ankles where the flow decelerates. On the other hand, the flow accelerates with a consequent decreased pressure in the external side of the feet. It is also revealed that a significant negative pressure area is detected in correspondence with the impact zone on feet and legs. The downstream vortical flow structure enhanced due to the intensified turbulence caused by the human obstacle. Figs. 12 shows the flow structure on staircase and amplified vortex near human body. Results indicate that when human on the rest platform, vortical flow structure in the vicinity of body from downstream steps enhanced by the intensified turbulence.

### 4.1.2. *Case 2: Human on the lower bench of the underground staircase*

Fig. 13 shows the configurations of human location on lower bench of the staircase. In this case, due to destroy of the relatively stable flow pattern on the platform, and the downstream lower bench of the staircase will produce a hydraulic jump region.

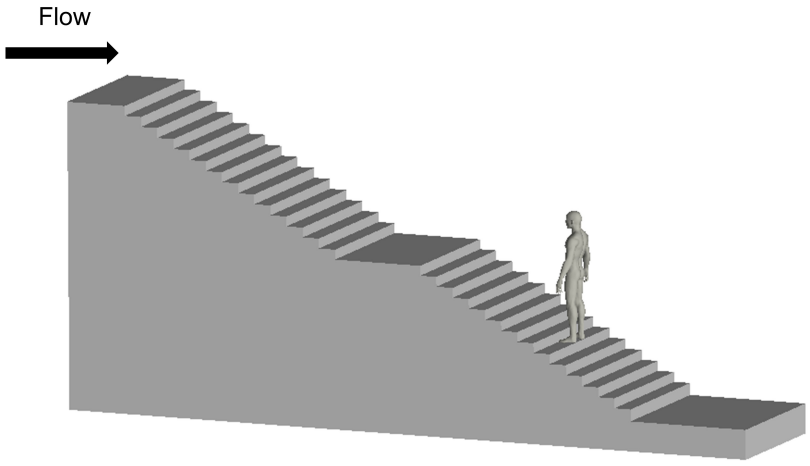


Figure 13: Schematic of human on the lower bench of the 8th step.

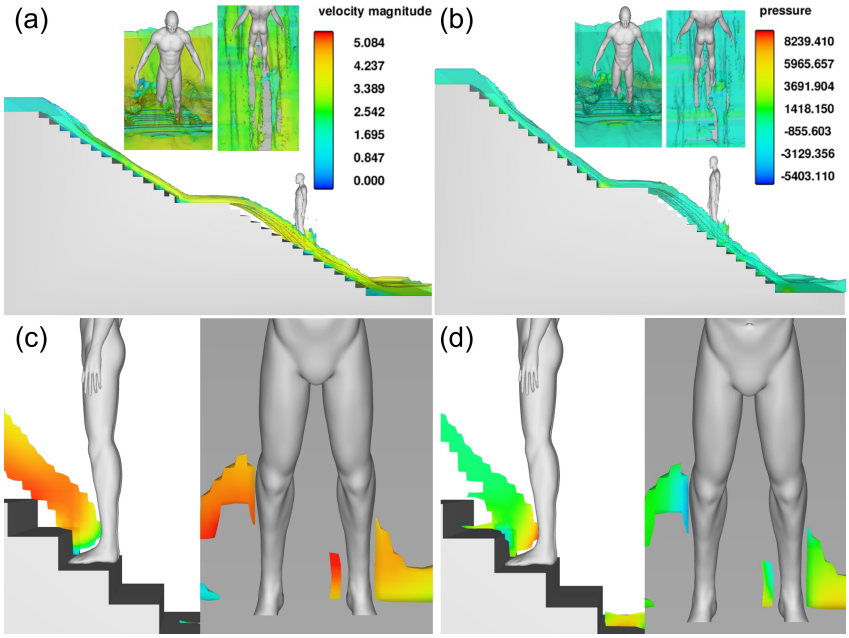


Figure 14: Flow structure including velocity and pressure of human on the 8th step in lower bench of the underground staircase. (a) distribution of velocity, (b) distribution of pressure, (c) amplified view of velocity in the vicinity of human body, (d) amplified view of pressure in the vicinity of human body

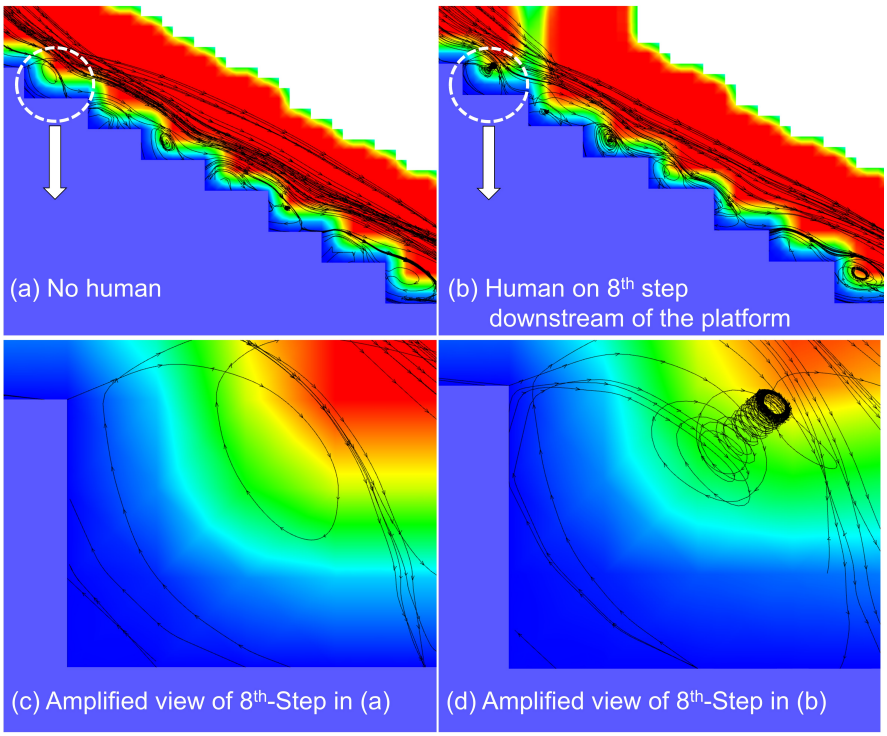


Figure 15: Flow streamline distribution in the lower bench of the staircase.(a) No human on the staircase, (b) Human on the lower bench, (c) Amplified view of flow streamline distribution near the 8-th step downstream of the platform in (a), (d) Amplified view of flow streamline distribution near the 8-th step downstream of the platform in (b).

Fig. 14 depicts the simulated flow with velocity magnitude and pressure distribution on the staircase and the amplified view of related results around the human body on the lower bench of the staircase. Downstream of the rest platform, a hydraulic jump occurs, the flow velocity increase dramatically in the jet drop and keep increasing after the jet plunges into the flow on the lower bench of the staircase. During this process, when the flow reaches to human on the 4-th step in the lower bench, the velocity significantly decreases while the pressure obviously increases. In addition, it is also observed that a significant splash area is detected in correspondence with the impact zone on feet and legs. The flow structure on staircase and amplified vortex near human body and the downstream vortical flow structure obviously enhanced because of the interdict of hydraulic jump by the human obstacle cause severe turbulence effect.

#### 4.1.3. Case 3: Human on the upper bench of the underground staircase

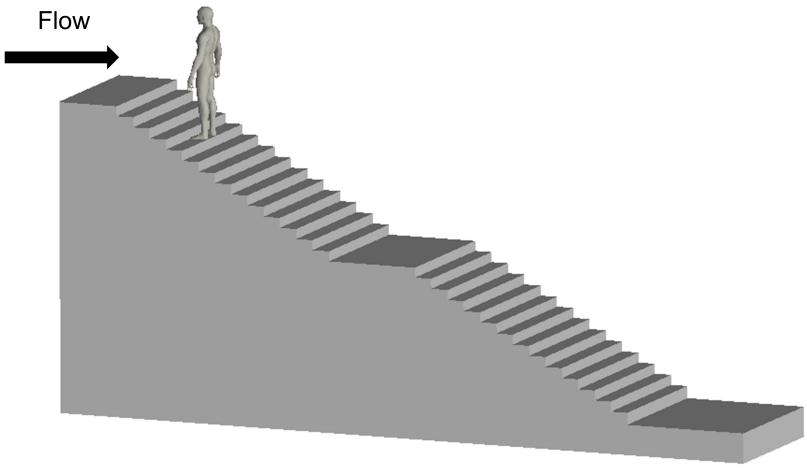


Figure 16: Schematic of human on the lower bench of the 8th step.

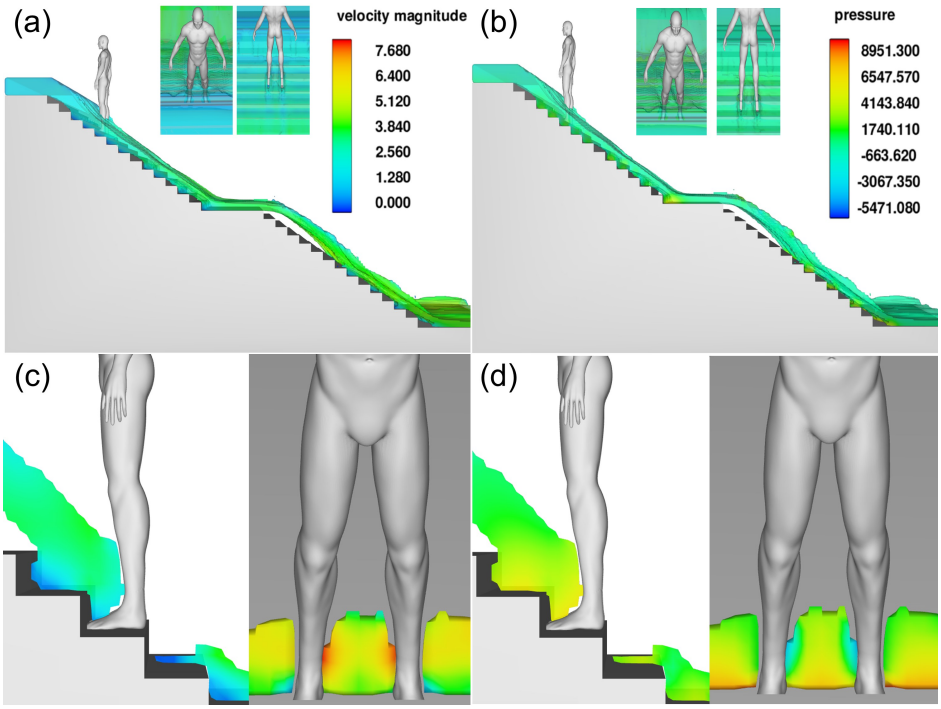


Figure 17: Flow structure including velocity and pressure of human on the 4th step in upper bench of the underground staircase. (a) distribution of velocity, (b) distribution of pressure, (c) amplified view of velocity in the vicinity of human body, (d) amplified view of pressure in the vicinity of human body

In this tested case, human is located on lower bench of the staircase in Fig. 16, where the speed of flow is relatively slow. Fig. 17 shows the simulated flow with velocity magnitude and pressure distribution on the staircase and the amplified view of related results around the human body located on the upper bench of the staircase. Once the flooding

water intrudes into the staircase, the flow velocity increase gradually and reach to a steady value along the staircase before the rest platform, which seems like a skimming flow (Gonzalez et al. 2008 Felder and Chanson, 2009 Takahashi and Ohtsu, 2013). The free surface elevation also decreases downstream after passing the ankles where the flow accelerates. The pressure increased above the ankles where the flow decelerates. On the other hand, the flow accelerates with a consequent decreased pressure in the inner and external side of the feet. This is different compared to human on the rest platform. Additionally, it is found that when human on upper bench, downstream vortical flow structures change slightly, because the flow speed on upper steps is slow the interaction influence of human body is relevantly small.

#### *4.1.4. Drag and lift coefficients*

Drag and lift coefficients are calculated by using Eq. (8) and Eq. (9) based on the mean values of integrated forces over the human geometry during the simulation and the frontal references areas $A$ in Table 1. Three experimental configurations of the physical model on human instabilities (Karvonen et al. 2000 Jonkman and Penning-Rowsell 2010, Xia et al. 2014b) are used.

Table 1: Physical characteristics of experimental human-scaled models and related frontal reference area.

| Experiments | (Karvonen et al. 2000) | (Jonkman and Penning-Rowsell 2010) | (Xia et al. 2014b) |
|---|---|---|---|
| $h_p(m)$ | 1.62 | 1.70 | 0.310 |
| $W(Kg)$ | 57.0 | 68.2 | 0.334 |
| $d(m)$ | 0.25 | 0.26 | 0.048 |
| $A(m^2)$ | 0.42 | 0.43 | 0.014 |

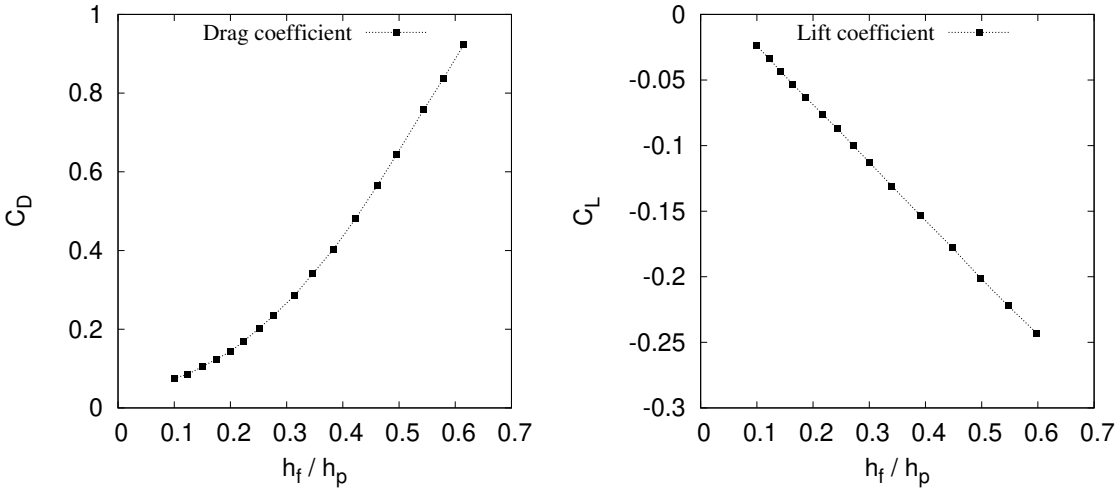


Figure 18: Drag and lift coefficients versus the relative submergence $h/h_p$ based on three experimental human-scaled models.

Fig. 18 depicts the fitted curves of drag and lift coefficients versus the relative submergence $h/h_p$ based on three experimental human-scaled models in Table 1. It is found that the drag coefficient increases exponentially while the lift coefficient decreased linearly with the submergence $h/h_p$. For both drag and lift coefficients, force coefficients in absolute value increase when submergence increased and the increment of drag coefficient is larger than that of lift coefficient.

### *4.2. Mechanics-based analysis for human instability in hydraulic jump region*

In this section, a mechanics-based analysis for human instability in hydraulic jump region is demonstrated based on the observation that significant flow deformation happened in the vicinity of hydraulic jump area. It is proved that when water flows through the intermediate rest platform, due to the sudden increase in the horizontal length, the relatively stable flow pattern is destroyed, and the downstream of the platform will produce a liquid jet. The step surface is exposed to the air, creating a hydraulic jump as shown in Fig. 19. It is found that in hydraulic jump region especially for the steps before the 5th-step, $\theta$ is smaller than the slope angle of the staircase ($26.6^o$). Here, recasting the critical condition for sliding instability as follows:

$$2\mu d\left(\frac{\rho_p}{\rho}-\frac{h_f}{h_p}\right)=\frac{U^2}{g}\left\{cos\theta\cdot(C_D+C_L)-sin\theta\cdot(C_D-C_L)\right\}. \tag{15}$$

For human stability condition, when $\theta$ decrease, $cos\theta$ increase and $sin\theta$ decrease, thus the right-hand side of Eq. (15) increase. However, in hydraulic jump region, the submergence $h/h_p$ increase and left-hand side of Eq. (15) decrease. As demonstrated in Sec. 4.1.4, $(C_D-C_L)$ and $(C_D+C_L)$ increase with the increase of $h/h_p$. Therefore, the potential of instability condition $2\mu d\left(\frac{\rho_p}{\rho}-\frac{h_f}{h_p}\right)<\frac{U^2}{g}\left\{cos\theta\cdot(C_D+C_L)-sin\theta\cdot(C_D-C_L)\right\}$ is higher in hydraulic jump region than other regions on the staircase, which may cause human sliding instability.

To evaluate the instability difference in hydraulic jump region for different age human, an adult as shown in Fig. 19 (a) and a child in Fig. 19 (b) are used to demonstrate the toppling instability analysis. Similarly, considering the critical condition for sliding instability in Eq. (15). Compared to an adult, the submergence a child $h/h_p$ is generally reduced

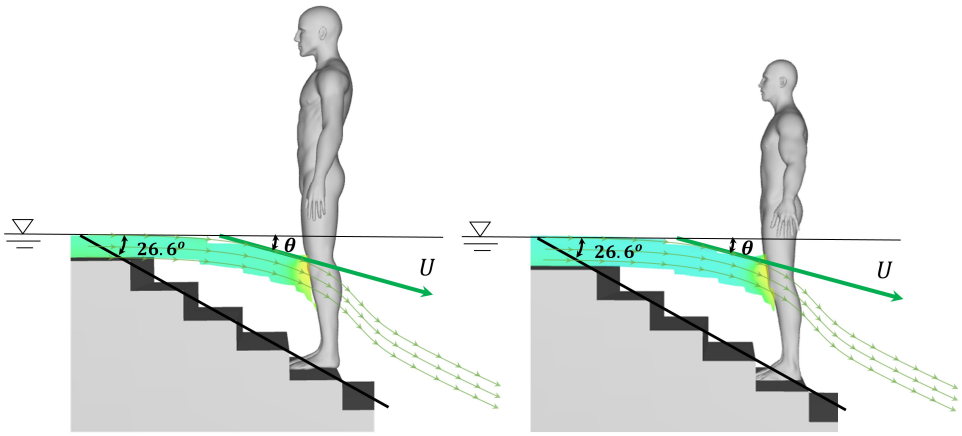


(a) Man in hydraulic jump area (4th step) (a) Boy in hydraulic jump area (4th step)

Figure 19: Simplified schematic of flow over human on the lower bench staircase

by about 10 to 40 percentages, which will cause an increased imbalance of Eq. (15) based on the above mechanics-based analysis. Therefore, the potential of topping instability condition for a boy is higher than an adult in hydraulic jump region. Numerically evaluated force coefficients and the mechanics-based analysis in hydraulic jump region for the occurrence of human instability indicates that human with large weight and height can reduce the risk of sliding instability.

### *4.3. Identification of hazard zones*

In this section, assessment of hazard zones are made to discuss the danger area on the staircase during flood events. Some representative risk index e. g. $f(U \cdot h_f)$ (Cox et al. 2010) or $f(U^2 \cdot h_f)$ (Ishigaki et al. 2006) can be used to classify different hazard zones, where $U$ is the water velocity and $h_f$ is the depth of the flow on the staircase. These empirical safety index formulae can quantitatively evaluate the evacuation risk by take into account the effects of water depth and velocity of water on the staircase.

In this work, the hazard zones are classified according to the critical safety index value $f(U^2 \cdot h_f) = 1.2\ m^3/s^2$ (Ishigaki et al. 2006) and $f(U^2 \cdot h_f) = 1.5\ m^3/s^2$ (Inoue et al. 2003), respectively. Lower risk zones are identified with the value $f(U^2 \cdot h_f)$ less than $1.2\ m^3/s^2$, and high risk zones are identified with the value $f(U^2 \cdot h_f)$ larger than $1.5\ m^3/s^2$. When $1.2\ m^3/s^2 < f(U^2 \cdot h_f) < 1.5\ m^3/s^2$, the zone is classified as a media risk.

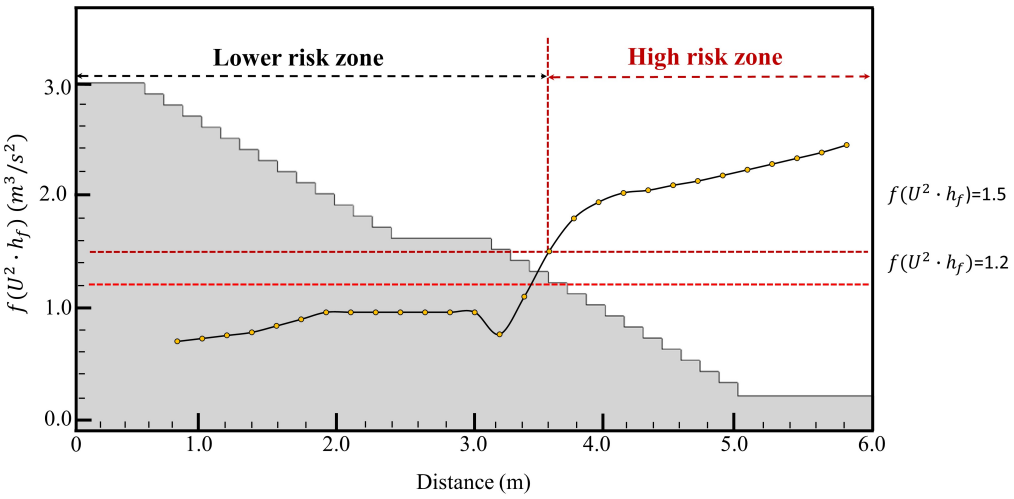


Figure 20: The trend of safety index $f(U^2 \cdot h_f)$ along the staircase.

Fig. 20 shows the distribution and the trend of safety index $f(U^2 \cdot h_f)$. It is observed that the magnitude of $f(U^2 \cdot h_f)$ increased steadily from the upper bench to the middle rest platform, and the value is less 1.2, which indicates the relatively lower risk zone. On the rest platform, the $f(U^2 \cdot h_f)$ declined due to the reduction of flow velocity. However, $f(U^2 \cdot h_f)$ shows a significant increase downstream of the rest platform due to the obviously increased velocity and water depth in the hydraulic jump region. Therefore, the existence of a hydraulic jump represents a relative high-risk zone, especially after the 3rd step downstream the rest platform.

## 5. Conclusions

This work was used for assessing metro flood risk, particularly focusing on human instability in different areas of the flooded metro staircase. The VOF method was used for simulating flood-prone region on staircase. The comparison between the experimental and numerical results demonstrates that the numerical simulation method can be used as a practical tool to obtain a reasonable assessment of human risk on flooded staircase incorporation with the mechanics-based instability analysis. Flow characteristic including velocity, pressure, and vortex distributions were obtained at first. Subsequently, a mechanics-based human instability analysis was conducted to make a qualitatively prediction of human risk in inundation metro staircase region. The conclusions are summarized as follows:

(1) Flow velocity on staircase increased gradually from the ground entrance to the underground exit. When water flows through the intermediate rest platform, due to the sudden increase in the horizontal length, the relatively stable flow pattern of falling water, transitional water and sliding water upstream of the platform is destroyed, and the downstream of the platform will produce a hydraulic jump.

(2) When human on the staircase, the following phenomena can be observed: (i) Free surface elevation increases upstream where the flow velocity reduces due to the obstruction of the human body. The pressure increased on the inner side of the feet and above the ankles where the flow decelerates. While flow accelerates with a consequent decreased pressure in the external side of the feet. (ii) A significant negative pressure area is detected in correspondence with the impact zone behind feet and legs. While the downstream flow is accelerated after passing the ankles where the flow accelerates. (iii) When human on the rest platform, vortical flow structure in the vicinity of body on downstream steps enhanced by the intensified turbulence. When human on lower bench, the downstream vortical flow structure obviously enhanced because of the interdict of hydraulic jump by the human obstacle cause severe turbulence effect. However, when human on upper bench, downstream flow structures change slightly, because the flow speed on upper steps is slow thus the interaction influence of human body is relevantly small.

(3) The most critical region of the studied case is identified where hydraulic jump happens, and the region especially after the 3rd step downstream of the hydraulic jump has a high potential to cause sliding instability. In addition, the risk of sliding instability for a boy is higher than that for an adult in hydraulic jump region.

(4) Overall, this is the first numerical investigation on the hydrodynamics and instability conditions of different human locations on the staircase in inundated metro station. The numerical model in this study can be applied to other types of metro staircases and metro systems. Based on the simulation results, the risk analysis and assessments can provide suggestive decision-making information in developing sustainable metro systems.

## Acknowledgments

This research work was supported by the National Natural Science Foundation of China (Grant Nos. 41890820, 51725902); the Royal Academy of Engineering through the Urban Flooding Research Policy Impact Programme (Grant No. UUFRIP/100031); and the Newton Advanced Fellowships from the NSFC and the UK Royal Society (Grant Nos. 52061130219; NAF/R1/201156).

## Data availability

The data that support the findings of this study are available from the corresponding author upon reasonable request.

## References


Abt, S. R., Wittier, R. J., Taylor, A., Love, D. J., 1989. Human stability in a high flood hazard zone1. Jawra Journal of the American Water Resources Association 25 (4), 881–890.

Arrighi, C., Oumeraci, H., Castelli, F., 2017. Hydrodynamics of pedestrians' instability in floodwaters. Hydrology And Earth System Sciences, 1–29.

Campisano, A., Butler, D., Ward, S., Burns, M. J., Friedler, E., Debusk, K., Fisher-Jeffes, L. N., Ghisi, E., Rahman, A., Furumai, H., 2017. Urban rainwater harvesting systems: Research, implementation and future perspectives. Water Research 121, 195.

Choi, Y., Kang, J., Kim, J., 2021. Urban flood adaptation planning for local governments: Hydrology analysis and optimization. International Journal of Disaster Risk Reduction 59, 102213.
URL https://www.sciencedirect.com/science/article/pii/S2212420921001795

Cox, R. J., Shand, T. D., Blacka, M. J., 2010. Australian rainfall and runoff revision project 10: Appropriate safety criteria for people.

Deng, Y., Cardin, M. A., Babouic, V., Santhanakrishnan, D., Schmittcr, P., Meshgi, A., 2013. Valuing flexibilities in the design of urban water management systems. Water Research 47 (20), 7162–7174.

Eini, M., Kaboli, H. S., Rashidian, M., Hedayat, H., 2020. Hazard and vulnerability in urban flood risk mapping: Machine learning techniques and considering the role of urban districts. International Journal of Disaster Risk Reduction 50, 101687.
URL https://www.sciencedirect.com/science/article/pii/S2212420920303484

Emanuelsson, M., Mcintyre, N., Hunt, C. F., Mawle, R., Kitson, J., Voulvoulis, N., 2014. Flood risk assessment for infrastructure networks. Journal of Flood Risk Management 7.

Falconer, R. A., Peng, G., Qian, C., Deng, S., Xia, J., 2015. Stability criterion for people in floods for various slopes. Water Management 169 (4), 1–10.

Felder, S., Chanson, H., 2009. Energy dissipation, flow resistance and gas-liquid interfacial area in skimming flows on moderate-slope stepped spillways. Environmental Fluid Mechanics 9 (4), 427–441.

Forero-Ortiz, E., Martnez-Gomariz, E., 2020. Hazards threatening underground transport systems. Natural hazards 100 (3), 1243 – 1261.

Gonzalez, C. A., Takahashi, M., Chanson, H., 2008. An experimental study of effects of step roughness in skimming flows on stepped chutes. Journal of Hydraulic Research 46 (sup1), 24–35.
URL https://doi.org/10.1080/00221686.2008.9521937

Hirt, C. W., Nichols, B. D., 1981. Volume of fluid (vof) method for the dynamics of free boundaries. Journal of Computational Physics 39, 201 – 225.
URL https://pdfs.semanticscholar.org/63af/0e90729f983539a0eaba62eaf04b61926a70.pdf

Inoue, K., Toda, K., Nakai, T., Takemura, N., Oyagi, R., 2003. On the inundation process in the underground space. Annuals of Disaster Prevention Research Institute, Kyoto University 47, 293–302.

Ishigaki, T., Kawanaka, R., Onishi, Y., Shimada, H., Toda, K., Baba, Y., 2009. Assessment of safety on evacuating route during underground flooding. In: Advances in Water Resources and Hydraulic Engineering. Springer Berlin Heidelberg, Berlin, Heidelberg, pp. 141–146.

Ishigaki, T., TODA, K., BABA, Y., INOUE, K., NAKAGAWA, H., 2006. Experimental study on evacuation from underground space by using real size models. PROCEEDINGS OF HYDRAULIC ENGINEERING 50, 583–588.

Jafari, A., Ashgriz, N., 2013. Numerical Techniques for Free Surface Flows: Interface Capturing and Interface Tracking. Springer US, Boston, MA, pp. 1–27.
URL https://doi.org/10.1007/978-3-642-27758-0_1139-2

Jiang, L. J., Shao, W. Y., Zhu, D. Z., Sun, Z. L., 2014. Forces on surface-piercing vertical circular cylinder groups on flooding staircase. Journal of Fluids and Structures 46, 17–28.

Jonkman, S., Penning-Rowsell, E., 2008. Human instability in flood flows1. JAWRA Journal of the American Water Resources Association 44 (5), 1208–1218.
URL https://onlinelibrary.wiley.com/doi/abs/10.1111/j.1752-1688.2008.00217.x

Jonkman, S. N., Penning-Rowsell, E., 2010. Human instability in flood flows1. Jawra Journal of the American Water Resources Association 44 (5), 1208–1218.

Kallianiotis, A., Papakonstantinou, D., Arvelaki, V., Benardos, A., 2018. Evaluation of evacuation methods in underground metro stations. International Journal of Disaster Risk Reduction 31, 526–534.
URL https://www.sciencedirect.com/science/article/pii/S2212420918302152

Karvonen, R. A., Hepojoki, A., Huhta, H. K., Louhio, A., 2000. The use of physical models in dam-break analysis.

Keller, R. J., Mitsch, B., 1993. Safety aspects of design roadways as floodways.

Kim, K., Ha, S., Kim, H., 2017. Using real options for urban infrastructure adaptation under climate change. Journal of Cleaner Production 143 (FEB.1), 40–50.

Kramer, M., Terheiden, K., Wieprecht, S., 2016. Safety criteria for the trafficability of inundated roads in urban floodings. International Journal of Disaster Risk Reduction 17, 77–84.
URL https://www.sciencedirect.com/science/article/pii/S2212420915301783

Li, Z., Zhang, X., Ma, Y., Feng, C., Hajiyev, A., 2019. A multi-criteria decision making method for urban flood resilience evaluation with hybrid uncertainties. International Journal of Disaster Risk Reduction 36, 101140.
URL https://www.sciencedirect.com/science/article/pii/S2212420919300056

Lind, N., Hartford, D., Assaf, H., 2004. Hydrodynamic models of human stability in a flood. Journal of the American Water Resources Association, 89–96.

Liu, S.-C., Peng, F.-L., Qiao, Y.-K., Zhang, J.-B., 2021. Evaluating disaster prevention benefits of underground space from the perspective of urban resilience. International Journal of Disaster Risk Reduction 58, 102206.
URL https://www.sciencedirect.com/science/article/pii/S2212420921001722

Lyu, Hai-Min, Sun, Wen-Juan, Shen, Shui-Long, Arulrajah, Arul, 2018. Flood risk assessment in metro systems of mega-cities using a gis-based modeling approach. Science of the Total Environment.

Lyu, H. M., Shen, S. L., Zhou, A., Yang, J., 2019. Perspectives for flood risk assessment and management for mega-city metro system. Tunnelling and Underground Space Technology 84 (FEB.), 31–44.

Lyu, H. M., Wang, G. F., Shen, J., Lu, L. H., Wang, G. Q., 2016. Analysis and gis mapping of flooding hazards on 10 may 2016, guangzhou, china. Water 8 (10), 447.

Motta, M., de Castro Neto, M., Sarmento, P., 2021. A mixed approach for urban flood prediction using machine learning and gis. International Journal of Disaster Risk Reduction 56, 102154.
URL https://www.sciencedirect.com/science/article/pii/S2212420921001205

Mugume, S. N., Gomez, D. E., Fu, G., Farmani, R., Butler, D., 2015. A global analysis approach for investigating structural resilience in urban drainage systems. Water Research 81, 15–26.

Noh, W., Woodward, P., 1976. Slic (simple line interface calculations). Proceedings of the Fifth International Conference on Numerical Methods in Fluid Dynamics 59, 330 – 340.

Park, K., hun Won, J., 2019. Analysis on distribution characteristics of building use with risk zone classification based on urban flood risk assessment. International Journal of Disaster Risk Reduction 38, 101192.
URL https://www.sciencedirect.com/science/article/pii/S2212420919301542

Peng, Jian, Fang-Le, 2018. A gis-based evaluation method of underground space resources for urban spatial planning: Part 1 methodology. TUNNELLING AND UNDERGROUND SPACE TECHNOLOGY.

Qiao, Y. K., Peng, F. L., Wang, Y., 2017. Monetary valuation of urban underground space: A critical issue for the decision-making of urban underground space development. Land Use Policy the International Journal Covering All Aspects of Land Use 69, pgs. 12–24.

Scardovelli, R., Zaleski, S., 1999. Direct numerical simulation of free-surface and interfacial flow. Annual Review of Fluid Mechanics 31, 567 – 603.
URL https://www.scopus.com/record/display.uri?eid=2-s2.0-0033489545&origin=inward&txGid=8f48191365bc16450ce95c7f868bae2b

Shao, W., Jiang, L., Fang, L., Zhu, D. Z., Sun, Z., 2015. Assessment of the safe evacuation of people walking through flooding staircases based on numerical simulation. Applied Physics and Engineering 16 (2), 117–130.

Shao, W., Xian, S., Lin, N., Small, M. J., 2017. A sequential model to link contextual risk, perception and public support for flood adaptation policy. Water Research 122 (oct.1), 216–225.

Shen, S. L., Wu, Y. X., Misra, A., 2017. Calculation of head difference at two sides of a cut-off barrier during excavation dewatering. Computers and Geotechnics 91, 192–202.

Singh, P., Sinha, V. S. P., Vijhani, A., Pahuja, N., 2018. Vulnerability assessment of urban road network from urban flood. International Journal of Disaster Risk Reduction 28, 237–250.
URL https://www.sciencedirect.com/science/article/pii/S2212420918303261

Sun, X., Li, R., Shan, X., Xu, H., Wang, J., 2021. Assessment of climate change impacts and urban flood management schemes in central shanghai. International Journal of Disaster Risk Reduction 65, 102563.
URL https://www.sciencedirect.com/science/article/pii/S2212420921005240

Takahashi, M., Ohtsu, I., 2013. Aerated flow characteristics of skimming flow over stepped chutes. Journal of Hydraulic Research 50 (4), 427–434.

Tan, Y., Lu, Y., 2018. Responses of shallowly buried pipelines to adjacent deep excavations in shanghai soft ground. Journal of Pipeline Systems Engineering and Practice 9 (2), 05018002.

Tan, Y., Zhu, H., Peng, F., Karlsrud, K., Wei, B., 2017. Characterization of semi-top-down excavation for subway station in shanghai soft ground. Tunnelling AND Underground Space Technology 68 (sep.), 244–261.

Tanir, T., Sumi, S. J., de Souza de Lima, A., de A. Coelho, G., Uzun, S., Cassalho, F., Ferreira, C. M., 2021. Multi-scale comparison of urban socio-economic vulnerability in the washington, dc metropolitan region resulting from compound flooding. International Journal of Disaster Risk Reduction 61, 102362.
URL https://www.sciencedirect.com/science/article/pii/S2212420921003289

Valdenebro, J., F.N. Gimena, F. L., 2019. Construction process for the implementation of urban utility tunnels in historic centres. Tunnelling and Underground Space Technology 89 (JUL.), 38–49.

Wu, Y. X., Lyu, H. M., Shen, J. S., Arulrajah, A., 2018. Geological and hydrogeological environment in tianjin with potential geohazards and groundwater control during excavation. Environmental Earth Sciences 77 (10), 392.

Xia, J., Falconer, R. A., Wang, Y., Xiao, X., 2014b. New criterion for the stability of a human body in floodwaters. Journal of Hydraulic Research 52 (1), 93–104.

Xia, J., Falconer, R. A., Xiao, X., Wang, Y., 2014a. Criterion of vehicle stability in floodwaters based on theoretical and experimental studies. Natural Hazards 70 (2), 1619–1630.

Xu, Y. S., Shen, S. L., Yue, L., Zhou, A. N., 2018. Design of sponge city: lessons learnt from an ancient drainage system in ganzhou, china. Journal of Hydrology 563, 900–908.

Yoneyama, N., Toda, K., Aihata, S., Yamamoto, D., 2009. Numerical analysis for evacuation possibility from small underground space in urban flood, 107–112.

Zhao, J. W., Peng, F. L., Wang, T. Q., Zhang, X. Y., Jiang, B. N., 2016. Advances in master planning of urban underground space (uus) in china. Tunnelling AND Underground Space Technology Incorporating Trenchless Technology Research 55 (may), 290–307.

Zhou, Z., James, A. S., Yanf, L., Baeck, M. L., Molly, C., Marie-Claire, T. V., Deng, H., Liu, S., 2017. The complexities of urban flood response: Flood frequency analyses for the charlotte metropolitan region. Water Resources Research 53, 7401–7425.

Zinda, J. A., Williams, L. B., Kay, D. L., Alexander, S. M., 2021. Flood risk perception and responses among urban residents in the northeastern united states. International Journal of Disaster Risk Reduction 64, 102528.
URL https://www.sciencedirect.com/science/article/pii/S2212420921004891